MEMBRANE TRANSPORT STRUCTURE FUNCTION AND BIOGENESIS:

Regulatory Interaction between the Cystic Fibrosis Transmembrane Conductance Regulator and HCO Salvage Mechanisms in Model Systems and the Mouse Pancreatic Duct

Wooin Ahn, Kyung Hwan Kim, Jin Ah Lee, Joo Young Kim, Joo Young Choi, Orson W. Moe, Sharon L. Milgram, Shmuel Muallem and Min Goo Lee

J. Biol. Chem. 2001, 276:17236-17243.
doi: 10.1074/jbc.M011763200 originally published online February 22, 2001

THE JOURNAL OF BIOLOGICAL CHEMISTRY
Vol. 276, No. 20, Issue of May 18, pp. 17236–17243, 2001

Printed in U.S.A.

Regulatory Interaction between the Cystic Fibrosis Transmembrane Conductance Regulator and HCO_3^- Salvage Mechanisms in Model Systems and the Mouse Pancreatic Duct*

Received for publication, December 28, 2000, and in revised form, February 6, 2001
Published, JBC Papers in Press, February 22, 2001, DOI 10.1074/jbc.M011763200

Wooin Ahn‡, Kyung Hwan Kim‡, Jin Ah Lee‡, Joo Young Kim‡, Joo Young Choi§, Orson W. Moe¶, Sharon L. Milgram‖, Shmuel Muallem§, and Min Goo Lee‡ ‡‡**

From the ‡Department of Pharmacology and Brain Korea 21 Project for Medical Sciences, Yonsei University College of Medicine, Seoul 120-752, Korea, the Departments of §Physiology and ¶Internal Medicine, University of Texas Southwestern Medical Center, Dallas, Texas 75235, and the ‖Department of Cell and Molecular Physiology, University of North Carolina, Chapel Hill, North Carolina 27599

The pancreatic duct expresses cystic fibrosis transmembrane conductance regulator (CFTR) and HCO_3^- secretory and salvage mechanisms in the luminal membrane. Although CFTR plays a prominent role in HCO_3^- secretion, the role of CFTR in HCO_3^- salvage is not known. In the present work, we used molecular, biochemical, and functional approaches to study the regulatory interaction between CFTR and the HCO_3^- salvage mechanism Na^+/H^+ exchanger isoform 3 (NHE3) in heterologous expression systems and in the native pancreatic duct. We found that CFTR regulates NHE3 activity by both acute and chronic mechanisms. In the pancreatic duct, CFTR increases expression of NHE3 in the luminal membrane. Thus, luminal expression of NHE3 was reduced by 53% in ducts of homozygote ΔF508 mice. Accordingly, luminal Na^+-dependent and HOE694-sensitive recovery from an acid load was reduced by 60% in ducts of ΔF508 mice. CFTR and NHE3 were co-immunoprecipitated from PS120 cells expressing both proteins and the pancreatic duct of wild type mice but not from PS120 cells lacking CFTR or the pancreas of ΔF508 mice. The interaction between CFTR and NHE3 required the COOH-terminal PDZ binding motif of CFTR, and mutant CFTR proteins lacking the C terminus were not co-immunoprecipitated with NHE3. Furthermore, when expressed in PS120 cells, wild type CFTR, but not CFTR mutants lacking the C-terminal PDZ binding motif, augmented cAMP-dependent inhibition of NHE3 activity by 31%. These findings reveal that CFTR controls overall HCO_3^- homeostasis by regulating both pancreatic ductal HCO_3^- secretory and salvage mechanisms.

Fluid secretion and the control of the ionic composition of biological fluids are essential for the function of many secretory epithelia, including the respiratory, digestive, and reproductive systems. HCO_3^- is an important constituent of secreted fluids by virtue of its function as the biological pH buffer and its effect on the solubility of proteins and ions in biological fluids. Accordingly, the mechanisms underlying HCO_3^- homeostasis at rest and during stimulation have attracted much attention in recent years. The importance of HCO_3^- homeostasis is evident from the marked reduction in Cl^-- and HCO_3^--dependent fluid secretion in the pancreatic juice of cystic fibrosis (CF)[1] patients (1).

CF is caused by mutations in the cystic fibrosis transmembrane conductance regulator (CFTR). CFTR functions as a Cl^- channel, and many mutations causing CF reduce or abolish Cl^- channel activity (2). However, several CFTR mutations retain normal or even elevated Cl^- channel activity although they are associated with mild or severe forms of CF (3). This suggests that CFTR may have other functions, besides conducting Cl^-, that are essential for normal fluid and electrolyte transport. Indeed, CFTR regulates the activity of the epithelial Na^+ channel ENaC (4), and CFTR supports Cl^-/HCO_3^- exchange activity in heterologous expression systems (5) and in the mouse pancreatic duct (6). Importantly, aberrant HCO_3^- transport in cells expressing CFTR mutants that retain Cl^- channel activity correlates with the pancreatic status of the CF phenotype (7). Another HCO_3^--transporting mechanism in tissues that express CFTR is HCO_3^--absorbing processes that may function as HCO_3^- salvage mechanisms in the resting state (8). In the pancreatic duct (8) and the kidney proximal tubule (9), 50% of HCO_3^- absorption is mediated by the Na^+/H^+ exchanger isoform 3 (NHE3) and 50% by a novel, yet unidentified, Na^+-dependent mechanism. Hence, HCO_3^- homeostasis in secretory epithelia is accomplished by both HCO_3^--absorbing (resting state) and HCO_3^--secretory (stimulated state) mechanisms.

An intriguing feature of HCO_3^- homeostasis is the possibility that the activity of multiple proteins involved in this process is regulated by CFTR through interaction with the scaffolding protein ERM (ezrin, radixin, moesin)-binding phosphoprotein 50 (EBP50) (also known as NHE-regulatory factor 1, or NHERF1). EPB50 has two PDZ domains and a C-terminal

* This work was supported by Basic Research Program of the Korea Science and Engineering Foundation Grant 2000-2-21400-002-1 (to M. G. L.) and National Institutes of Health Grants DE12309 and DK38938 (to S. M.) and HL63755 (to S. L. M.). The costs of publication of this article were defrayed in part by the payment of page charges. This article must therefore be hereby marked "*advertisement*" in accordance with 18 U.S.C. Section 1734 solely to indicate this fact.

The nucleotide sequence(s) reported in this paper has been submitted to the GenBank™/EBI Data Bank with accession number(s) AF307992 and AF307993.

** To whom correspondence may be addressed: Dept. of Physiology, University of Texas Southwestern Medical Center, 5323 Harry Hines Blvd., Dallas, TX 75235-9040. Tel.: 214 648 2593; Fax: 214 648 8879; E-mail: Shmuel.Muallem@UTSouthwestern.edu.

‡‡ To whom correspondence may be addressed: Dept. of Pharmacology, Yonsei University College of Medicine, 134 Sinchon-Dong, Seoul 120-752, South Korea. Tel.: 82 2 361 5221; Fax: 82 2 313 1894; E-mail: mlee@yumc.yonsei.ac.kr.

[1] The abbreviations used are: CF, cystic fibrosis; CFTR, cystic fibrosis transmembrane conductance regulator; NHE, Na^+/H^+ exchanger; EBP50, ERM-binding phosphoprotein 50; BCECF, 2′7′-bis-(2-carboxyethyl)-5-(and-6)-carboxyfluorescein; AM, acetoxymethyl ester; PCR, polymerase chain reaction; RT-PCR, reverse transcription-PCR; WT, wild type; ΔF, ΔF508; LM, luminal membrane; VIP, vasoactive intestinal polypeptide.

ERM binding domain. Separate reports showed that the first PDZ domain of EBP50 preferentially binds the C terminus of CFTR (10) and that NHE3 interacts with EBP50 via a nontraditional association that requires the second PDZ domain and the C terminus of EBP50 (11). Likewise, CFTR and NHE3 both associate with the closely related protein E3KARP (12). NHE3 activity is acutely inhibited by cAMP-dependent phosphorylation, and EBP50 or E3KARP is required to mediate this inhibition, perhaps by binding to ezrin, which may function as a protein kinase A anchoring protein (13). Since both CFTR and NHE3 can associate with EBP50 and cAMP regulates both activities, we considered the possibility that CFTR modulates the activity of NHE3 by association with EBP50 or other related proteins (13, 14). In this manner, CFTR can regulate not only HCO_3^- secretion but also HCO_3^- salvage.

In the present work, we used biochemical and functional approaches to study the interaction of CFTR and NHE3 with EBP50 and the functional significance of this interaction in heterologous expression systems and the native pancreatic duct. In pancreatic duct and PS120 cells expressing NHE3 and EBP50, expression of CFTR augmented the cAMP-dependent inhibition of NHE3 activity. Most notably, CFTR in the pancreatic duct affected not only the activity but also the expression of NHE3 protein in the luminal membrane. These findings reveal a new mechanism by which CFTR regulates ion transport at the luminal membrane and highlight the multiple functions of CFTR in regulating the overall HCO_3^- homeostasis in the pancreatic duct and possibly in other CFTR-expressing epithelia.

EXPERIMENTAL PROCEDURES

Materials, Antibodies, and Solutions—BCECF-AM was purchased from Molecular Probes, Inc. (Eugene, OR). Polyclonal antiserum directed against human EBP50 was generated in rabbits as described previously (15). Rabbit antisera 1566 and 1568 specific for NHE3 were generated as described previously (16). Monoclonal antibodies against an R domain and a C terminus of CFTR were purchased from R & D Systems (Minneapolis, MN). The solution A, used for microdissection and perfusion, contained (in mM) 140 NaCl, 5 KCl, 1 $MgCl_2$, 1 $CaCl_2$, 10 HEPES (pH 7.4 with NaOH), and 10 glucose. Na^+-free solutions were prepared by replacing Na^+ with *N*-methyl-D-glucamine$^+$ from solution A.

Cell Culture and Transfection—An NHE-deficient cell line PS120, originally developed by Pouyssegur *et al.* (17), and the pCMV-NHE3 mammalian expression vector (18) were provided by Drs. K. Park and J. E. Melvin (University of Rochester). Mammalian expressing pCMV-CFTR (pCMVNot6.2) vector was a gift from Dr. J. Rommens at the Hospital for Sick Children (Toronto, Canada). Mammalian expressing Ad-CFTR virus was purchased from the Institute of Human Gene Therapy (Philadelphia, PA), and pcDNA3.1-EBP50 was generated by subcloning the full-length EBP50 cDNA from pET-EBP50 (15) to pcDNA3.1 (Invitrogen, Groningen, The Netherlands).

PS120 cells were maintained in DMEM-HG (Life Technologies, Inc.) supplemented with 10% fetal bovine serum and penicillin (50 units/ml)/streptomycin (50 μg/ml). The pCMV-NHE3 construct was stably transfected into a PS120 cell line using LipofectAMINE Plus Reagent (Life Technologies). NHE3 stable transfectants (PS120/NHE3) were selected by resistance to the antibiotic Geneticin (G418; Life Technologies, Inc.) and by an H^+-killing method (19).

Site-directed Mutagenesis—Oligonucleotide-directed mutagenesis using the GeneEditor mutagenesis kit (Promega, Madison, WI) was performed in the CFTR expression vector pCMVNot6.2 to delete the C-terminal 4 (ΔDTRL) or 26 (S1455X) amino acids. Briefly, mutants were selected based upon the incorporation of a second-site mutation in β-lactamase, which alters its substrate specificity, allowing resistance of transformed bacteria to cefotaxime and cerftriaxone in addition to ampicillin. Incorporation of the mutation was verified by DNA sequencing. The mutagenesis primers were as follows: ΔDTRL, 5′-GGA GAC AGA AGA AGA GGT G**TA AG**A TAC AAG GCT TTA GAG AG-3′; S1455X, 5′-GCT CTT TCC CCA CCG GAA C**TG AG**AG CAA GTG CAA GTC TAA GCC-3′.

RT-PCR—mRNA transcripts of mouse EBP50, E3KARP, and PDZK1 (20) were analyzed in pancreatic and PS120 cells using RT-PCR. Among several primer sets designed based on the mouse sequences, at least one set for each protein detected the correct band in samples from hamster as well as mouse tissues. The primer sequences were as follows: 1) mEBP50, sense (5′-CTA AGC CAG GCC AGT TCA TCC GAG CAG T-3′) and antisense (5′-TGG GGT CAG AGG AGG AGG AGG AGG TAG A-3′), size of PCR product 447 base pairs; 2) mE3KARP, sense (5′-GAG GCC CGG CTG CTG GTA GTC G-3′) and antisense (5′-CAT CTG TGG TGC CCG CTT GTT GA-3′), size of PCR product 312 base pairs; 3) mPDZK1, sense (5′-GAC AAG GCT GGG CTG GAG AAT GAG GAC-3′) and antisense (5′-CGA AGA GTG CGA GGC TGT GCT GAG AGT-3′), size of PCR product 297 base pairs. RNA was extracted from the tissue using Trizol solution (Life Technologies, Inc.) and reverse transcribed using random hexamer primers and an RNase H^- reverse transcriptase (Life Technologies). The cDNA was amplified using specific primers and a *Taq* polymerase (Promega), and the products were separated on a 1.5% agarose gel containing 0.1 μg/ml ethidium bromide. The identities of all amplified products were verified by nucleotide sequencing.

Immunoprecipitation and Immunoblotting—Precleared pancreatic or PS120 lysates (~2 mg of protein) were mixed with the appropriate antibodies and incubated overnight at 4 °C in lysis buffer. Immune complexes were collected by binding to protein G- (monoclonal antibody against R domain of CFTR) or protein A- (all other antibodies) Sepharose and washing four times with lysis buffer prior to electrophoresis. The immunoprecipitates or lysates (20 μg of protein) were suspended in SDS sample buffer and separated by SDS-polyacrylamide gel electrophoresis. The separated proteins were transferred to polyvinylidene difluoride membranes, and the membranes were blocked by a 1-h incubation at room temperature in 5% nonfat dry milk in a solution containing 20 mM Tris-HCl, pH 7.5, 150 mM NaCl, and 0.05% Tween 20. The proteins were detected by 1-h incubations with the appropriate primary and secondary antibodies.

Immunohistochemistry and Quantitation of Staining in Confocal Images—The pancreata from several wild type (WT) and homozygous ΔF508 (ΔF) mice were embedded in OCT (Miles, Elkhart, IN), frozen in liquid N_2, and cut into 4-μm sections. Immunostaining of frozen sections was performed as previously reported (8). Briefly, the sections were fixed and permeabilized by incubation with cold methanol for 10 min at −20 °C. After removal of the methanol, slices were washed twice with phosphate-buffered saline, and the tissue area was encircled using a hydrophobic marker (Pap Pen; Zymed Laboratories Inc., South San Francisco, CA). Nonspecific binding sites were blocked by incubation for 1 h at room temperature with 0.1 ml of phosphate-buffered saline containing 5% goat serum, 1% bovine serum albumin, and 0.1% gelatin (blocking medium). After blocking, the sections were stained by incubation with the appropriate primary antiserum followed by fluorophore-tagged secondary antibodies. For double labeling experiments, these primary and secondary incubations were repeated with antibodies against the second protein of interest. Then the sections were incubated in a bisbenzimide (10 μg/ml in phosphate-buffered saline) solution to stain DNA and sealed with a coverslip using a Mowiol-based (Calbiochem) mounting medium. Images were collected with a Leica TCS-NT confocal microscope.

When desired, NHE3 expression in the LM of the pancreatic duct was compared between samples from wild type and ΔF mice. In this case, all of the images were taken at the same laser intensity, and the same recording conditions and staining intensities of specified regions were analyzed using an imaging software (MCID version 3.0; Brook University, St. Catharines, Ontario, Canada). Briefly, the pixel counts of a 1-μm square region in the nucleus (F_{Nuc}; background) and a midportion of the LM (F_{LM}) of the same cell were measured. The ratio of $(F_{LM} - F_{Nuc})/F_{Nuc}$ from multiple cells taken from at least three separate sections and from separate animals were averaged and compared between each group.

Animals and Preparation of Pancreatic Ducts—A cystic fibrosis mouse model in which the ΔF508 mutation was introduced in the mouse CFTR gene targeting in embryonic stem cells (21) was obtained from Dr. K. R. Thomas (University of Utah). The mice were maintained on a standard diet, and genotyping was carried out during days 7–14 postpartum, as described (22). The procedure for preparation and perfusion of the main pancreatic duct was identical to that described previously (8). Briefly, the mice were anesthetized, the abdomen was opened, and the duct lumen was cannulated using a modified 31-gauge needle. After ligating the proximal end of the common duct, the pancreas was removed into a dish containing ice-cold solution A supplemented with 0.02% soybean trypsin inhibitor and 0.1% bovine serum albumin. The main duct was cleared of acini and connective tissue, and the proximal end of the main duct was cut in order to facilitate retrograde luminal perfusion. After transferring to the perfusion chamber and during pH_i measurement, the ducts were continuously perfused with separate bath

and luminal solutions.

Intracellular pH Measurements—For measurement of pH_i in PS120/NHE3 cells, the glass coverslips with cells attached to them were washed once with solution A and assembled to form the bottom of a perfusion chamber. The cells were loaded with BCECF by a 10-min incubation at room temperature in solution A containing 2.5 μM BCECF-AM. After dye loading, the cells were perfused with appropriate solutions, and pH_i was measured by photon counting using a fluorescence measuring system (Delta Ram; PTI Inc., South Brunswick, NJ). In the case of CFTR transfection with pCMVNot6.2 or its C-terminal deleted mutants, a green fluorescent protein-expressing plasmid (Life Technologies) was co-transfected with the CFTR constructs, and pH_i measurements were performed with cells expressing high levels of green fluorescent protein as previously reported (5). For pH_i measurement in the microdissected ducts, the cannulated ducts were transferred to a perfusion chamber placed on the stage of an inverted microscope. The bath was perfused at a flow rate of 6 ml/min, and the lumen was perfused at a flow rate of 150 μl/min using solution A that was maintained at 37 °C. BCECF was loaded by including 2.5 μM BCECF-AM in the luminal perfusate for 5 min, and dye loading was monitored. After completion of dye loading, the lumen was washed by perfusing solution A, and pH_i measurements were performed according to the specified protocols. The fluorescence ratios of 490/440 nm were calibrated intracellularly by perfusing the cells or the ducts with solutions containing 145 mM KCl, 10 mM HEPES, and 5 μM nigericin with pH adjusted to 6.2–7.8.

Na^+/H^+ exchange activity was measured using a standard protocol (23). The cells were acidified by an NH_4^+ pulse and subsequent perfusion with a Na^+-free solution. The maximal Na^+-dependent pH_i recovery was measured in cells acidified to pH_i 6.4–6.5. Buffer capacity was calculated by measuring ΔpH_i in response to 5–20 mM NH_4Cl pulses. In each experiment, the buffer capacity (β_i) showed a negative linear relationship with pH_i between 6.4 and 7.3. The β_i of PS120 cells (30.2 ± 2.1 mM/pH unit at pH_i 7.0) was lower than that of the pancreatic duct cells (48.6 ± 6.2). However, forskolin treatment or any gene modulation did not significantly change β_i. Therefore, all the results of NHE activity are expressed as ΔpH/min, and this value was directly analyzed without compensating for β_i. The results are presented as mean ± S.E., and, when appropriate, statistical analysis was determined using Student's *t* test or analysis of variance. $p < 0.05$ was considered statistically significant.

RESULTS

CFTR·EBP50·NHE3 Complexes in PS120 Cells and the Mouse Pancreas—To set the stage for analyzing the interaction between CFTR and NHE3 in model systems and native cells, we first determined which of the adapter proteins known to interact with CFTR are expressed in these cells (10, 12). These include EBP50 and E3KARP, both of which contain two PDZ domains and associate with ezrin via the C terminus. We also examined the expression of the related mRNA encoding PDZK1 (also called CAP70), a protein that contains four PDZ domains (20). Although PDZK1 is known to associate with CFTR (24), it is not known whether it also associates with NHE3 or ezrin via an ERM binding domain. The RT-PCR analysis shown in Fig. 1*A* reveals expression of mRNA for EBP50, E3KARP (13), and PDZK1 (20) in hamster lung and the mouse pancreas. On the other hand, only mRNA for EBP50 was detected in PS120 cells.

Expression of EBP50 in PS120 cells was unexpected, since a previous study reported that this cell line does not express EBP50 (13). To substantiate the RT-PCR findings, expression of EBP50 in the hamster fibroblast-derived PS120 clone was first verified by sequencing the amplified RT-PCR product. As shown in Fig. 1*B*, EBP50 in PS120 cells showed the highest similarity to Chinese hamster EBP50 with 99% homology based on nucleotide sequences (GenBank™ accession numbers AF307992 and AF307993). The 1% sequence difference is probably due to the use of mutagenic agents during the selection of the NHE-deficient cells (17) or due to substrain differences. Expression of EBP50 protein in our PS120 cells was examined by Western blotting using a polyclonal antiserum generated against full-length human EBP50. Fig. 1*C* shows expression of EBP50 protein in both PS120 cells and the mouse pancreas.

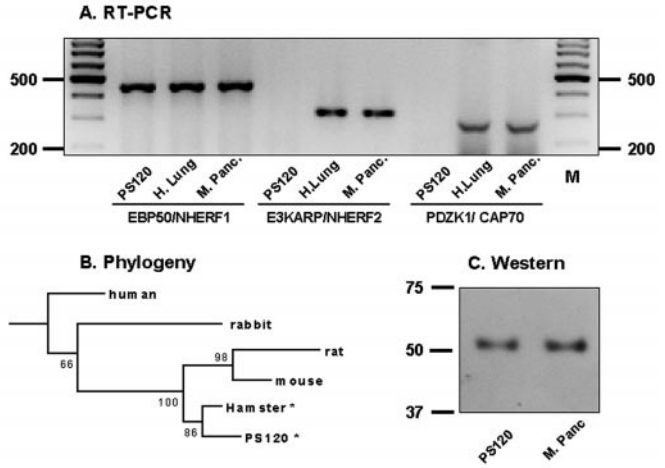

FIG. 1. **Expression of EBP50 in PS120 cells and the mouse pancreas.** *A*, mRNA was prepared from PS120 cells, Chinese hamster lung (*H. Lung*), and the mouse pancreas (*M. Panc.*), and primers listed under "Experimental Procedures" were used to amplify a sequence from EBP50, E3KARP, and PDZK1 from all mRNA preparations. *B*, phylogenetic analysis of EBP50 expressed in the five species indicated in the tree and in PS120 cells. The 408-base pair nucleotide sequences (corresponding to 672–1079 of mouse EBP50) were aligned, and a neighbor-joining tree was drawn. The bootstrap probabilities, as determined for 1000 resamplings, are given in percentages *beside* the internal branches. *, the sequences of PS120 (GenBank™ accession number AF307992) and hamster (AF307993) were sequenced in this study, and others were selected from registered sequences in GenBank™ (human, NM004252; rabbit, U19815; rat, AF154336; mouse, U74079). *C*, Western blot analysis of EBP50 in lysates prepared from PS120 cells and the mouse pancreas.

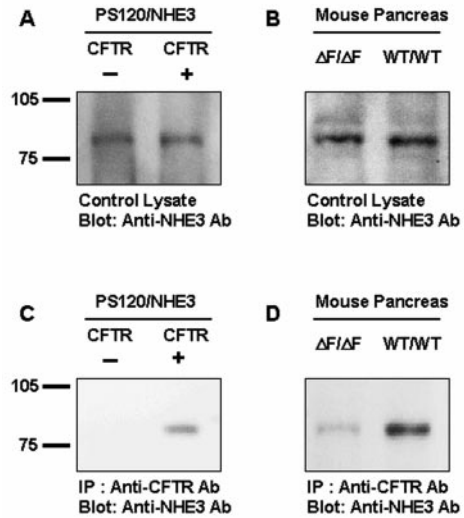

FIG. 2. **Immunoprecipitation of CFTR·NHE3 complexes from PS120 cells and the mouse pancreas.** Lysates were prepared from PS120/NHE3, PS120/NHE3 infected with Ad-CFTR (*A*), and the pancreas of WT and ΔF508 mice (*B*). The lysates were analyzed by blotting with NHE3 antisera to ensure the same amount of NHE3 protein in the extracts during immunoprecipitation (*A* and *B*). For immunoprecipitation, precleared extracts from PS120/NHE3 or the mouse pancreas were incubated with monoclonal antibodies recognizing the R domain of CFTR. The immunoprecipitates were separated by SDS-polyacrylamide gel electrophoresis, transferred to membrane, and blotted with the anti-NHE3 antibody 1568 (PS120/NHE3 cells (*C*) and pancreatic extracts (*D*)). *IP*, immunoprecipitation.

Previous works reported that EBP50 can associate with CFTR or NHE3 (10, 11). We first confirmed these findings in our PS120 cells that were transfected with either CFTR or NHE3 (not shown). Subsequently, we asked whether CFTR and NHE3 exist in the same complex when expressed in PS120

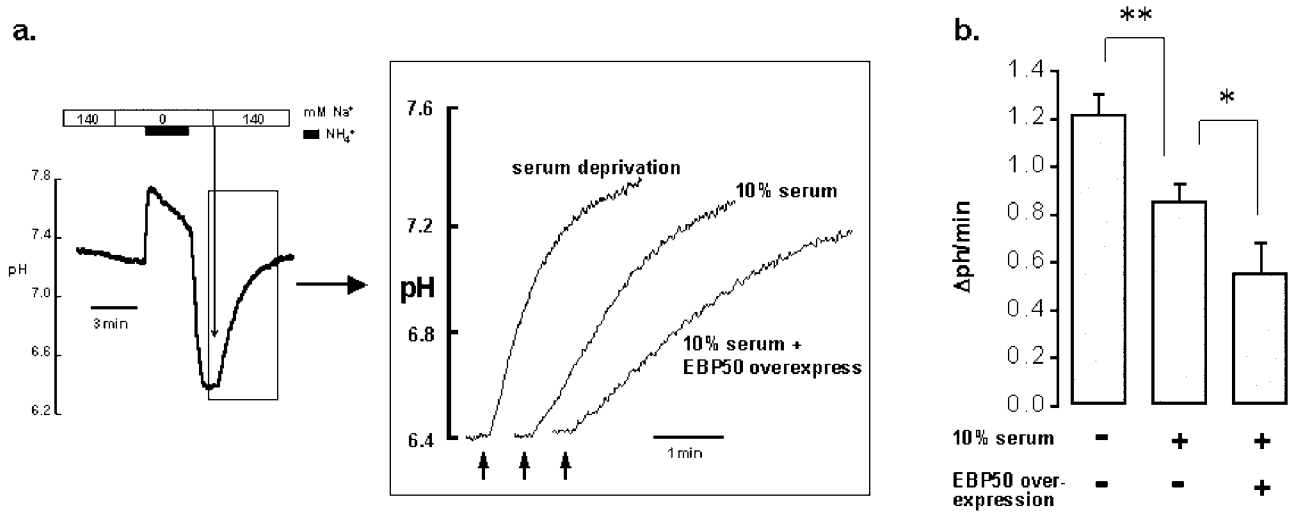

FIG. 3. **Effect of serum deprivation and overexpression of EBP50 on NHE3 activity in PS120/NHE3 cells.** PS120/NHE3 cells were serum-deprived or transfected with EBP50. The experimental protocol of acidifying cells with an NH_4^+ pulse in Na^+-free medium to measure NHE3 activity and examples of individual experiments are shown in *A*. *B* shows the summary of seven, nine, and six experiments performed with serum-deprived, control, and EBP50-overexpressing cells, respectively. **, $p < 0.01$; *, $p < 0.05$ compared with control.

cells and in the *in vivo* situation. For these experiments, NHE3 was stably expressed in PS120 cells to generate the PS120/NHE3 clone, and a portion of PS120/NHE3 cells was infected with Ad-CFTR. The blot in Fig. 2*A* shows that expression of CFTR had no measurable effect on expression of NHE3 protein in PS120/NHE3 cells. Lysates were prepared from control and CFTR-expressing PS120/NHE3 cells, and an antibody recognizing the R domain of CFTR was used to immunoprecipitate CFTR from PS120/NHE3 cells and PS120/NHE3 cells co-expressing CFTR. NHE3 was found in the CFTR immunoprecipitates from the cells infected with Ad-CFTR (Fig. 2*C*), demonstrating that exogenously expressed CFTR and NHE3 may associate in a stable complex in PS120 cells.

To determine whether CFTR and NHE3 also associate in native cells, we performed similar experiments using mouse pancreata from WT and ΔF mice. For these experiments, the amount of lysate used was adjusted to contain the same amount of NHE3 (Fig. 2*B*). NHE3 was found in CFTR immunoprecipitates from the pancreas of WT mouse (Fig. 2*D*). In contrast, only a very small amount of NHE3 was found in CFTR immunoprecipitates from the pancreas of ΔF mouse. The small amount of NHE3 found to associate with ΔF508 CFTR can be accounted for by the small amount of CFTR that is found in the luminal membrane of these mice (22). The findings in Fig. 2 provide the first evidence that NHE3 and CFTR exist in the same multiprotein complex, both in model systems and in native cells.

Functional Interaction between CFTR and NHE3—To study the effect of CFTR on NHE3 activity, we first determined the optimal conditions to study this interaction. In previous work, the cAMP-dependent and EBP50-mediated inhibition of NHE3 activity was studied in serum-deprived, G_o/G_1-arrested PS120 cells that were transfected with EBP50 (13). Fig. 3 shows the results of similar experiments in our PS120/NHE3 cells. Serum deprivation for 18 h increased NHE3 activity by ~41%. This is attributable to an increase in NHE3 expression under these conditions.[2] Exogenous overexpression of EBP50 in PS120/NHE3 cells reduced NHE3 activity in unstimulated cells by ~35%. Preliminary studies showed that the optimal experimental condition to consistently observe regulation of NHE3 by CFTR is to maintain the PS120/NHE3 cells in 10% serum and to rely on the EBP50 already expressed in the cells.

Having established optimal conditions for measuring NHE3 activity in PS120 fibroblasts, we next examined the effect of increased cAMP on NHE3 activity of control PS120/NHE3 cells and cells transfected with CFTR (Fig. 4). Treatment of PS120/NHE3 cells with forskolin dose-dependently inhibited NHE3 activity. At 0.1 and 10 μM forskolin, NHE3 activity of PS120/NHE3 cells was 91.6 ± 6.1 and 70.8 ± 5.1% of control, respectively. Importantly, expression of CFTR had no effect on basal NHE3 activity (rates of pH_i recovery: 0.86 ± 0.09 ΔpH/min ($n = 6$) in control and 0.94 ± 0.10 ΔpH/min ($n = 9$) in CTFR-expressing PS120/NHE3 cells). Incubation of CFTR-expressing PS120/NHE3 cells with forskolin also inhibited NHE3 activity in a dose-dependent manner. However, the inhibition was nearly maximal at 0.1 μM forskolin; at 0.1 and 10 μM forskolin, NHE3 activity in CFTR-expressing cells was 60.3 ± 5.1 and 53.4 ± 6.2% of control, respectively. Thus, we conclude that activation of CFTR augments cAMP-mediated inhibition of NHE3.

Fig. 4 shows that CFTR markedly augments the inhibition of NHE3 by cAMP. CFTR binds to EBP50 through its C-terminal DTRL sequence, a signature PDZ domain-binding motif (10). Therefore, we examined whether the enhanced cAMP-dependent inhibition of NHE3 required association of CFTR with PDZ-containing scaffolding proteins. Fig. 5 provides biochemical and functional evidence that the COOH terminus of CFTR is required for association of CFTR with NHE3 in the same multiprotein complex. Thus, when we expressed CFTR mutants lacking the final 4 amino acids involved in binding PDZ proteins (ΔDTRL), CFTR and NHE3 were no longer co-immunoprecipitated (Fig. 5, *A* and *B*). Furthermore, in cells expressing CFTR-ΔDTRL, activation of CFTR with forskolin did not augment the cAMP-mediated inhibition of NHE3 (Fig. 5*C*). It is important to note that deletion of the DTRL sequence has no effect on the function of CFTR as a Cl^- channel (25). Another finding of note in Fig. 5 is the behavior of a mutant CFTR protein lacking the final C-terminal 26 amino acids (S1455X). This mutation, which is associated with impaired fluid secretion (26), appears to have no effect on CFTR Cl^- channel activity (25) but rather results in inefficient targeting of CFTR to the luminal membrane of polarized cells (27). Similar to the findings with the CFTR-ΔDTRL, the CFTR-S1455X did not associate with NHE3 (Fig. 5*B*) and had no effect on NHE3 activity (Fig. 5*C*). Taken together, these data indicate that CFTR and NHE3 exist within a multiprotein com-

[2] O. W. Moe, unpublished observation.

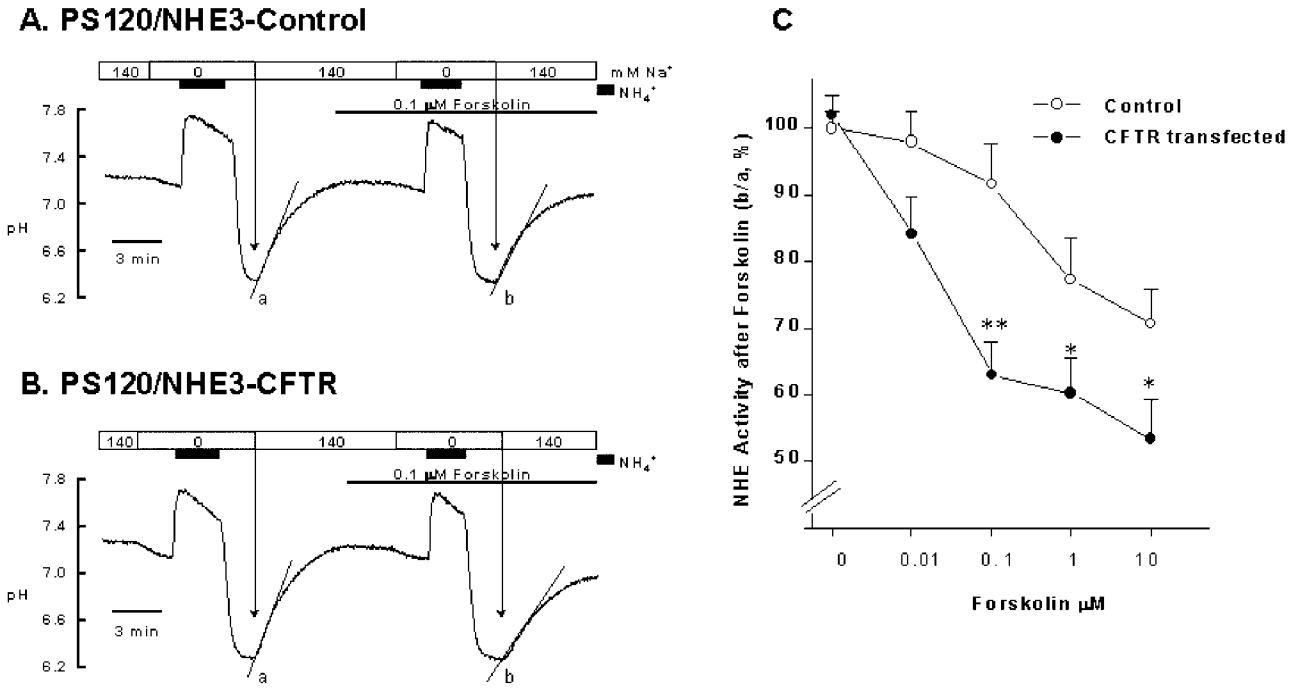

FIG. 4. **Expression of CFTR augments cAMP-mediated inhibition of NHE3 activity in PS120/NHE3 cells.** PS120/NHE3 cells infected with Ad-LacZ (*A*, control) or Ad-CFTR (*B*) were acidified twice, before and after stimulation with forskolin, and Na^+-dependent pH recovery from acidification was measured. The ratios of the slopes of forskolin-stimulated to control periods (*b*/*a*) were calculated and plotted in *C* to evaluate the effect of CFTR on NHE3 activity. Stimulation of CFTR with 0.1 μM forskolin and above significantly inhibited NHE3 activity beyond that observed in control cells. **, $p < 0.01$; *, $p < 0.05$ compared with control.

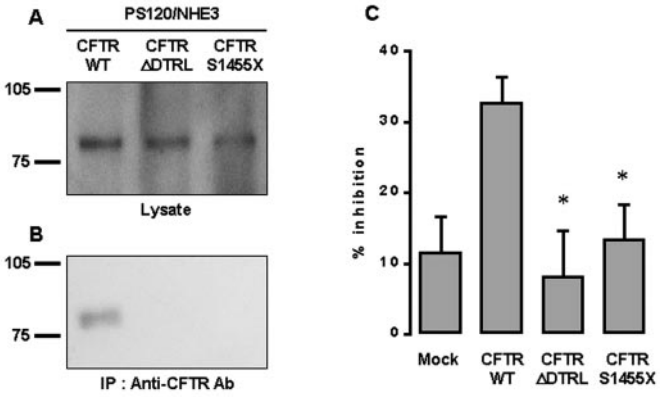

FIG. 5. **The C terminus of CFTR is required for formation of CFTR·NHE3 complexes and regulation of NHE3 activity by CFTR.** PS120/NHE3 cells were transfected with mammalian expressing vectors for WT-CFTR, CFTR-ΔDTRL, and CFTR-S1455X. Lysates were prepared from all cells, and lysates containing an equal amount of CFTR constructs (*A*) were used to immunoprecipitate (*IP*) CFTR with antibodies recognizing the R domain of CFTR (*B*). The same cells were used to measure the effect of cAMP stimulation (0.1 μM forskolin) on NHE3 activity using protocols in Fig. 4 (*C*). *, $p < 0.05$ compared with control.

plex in PS120 cells. Furthermore, the data indicate that binding of CFTR to EBP50 (or other EBP50-related protein) is required for association of CFTR with NHE3 and for CFTR-mediated inhibition of NHE3.

Biochemical and Functional Association of CFTR with NHE3 in the Mouse Pancreatic Duct—CFTR and NHE3 association in the pancreas of WT but not ΔF mice (Fig. 2) suggested that the two proteins exist in the same complex and are co-localized in the pancreatic duct. This prediction was verified by immunolocalization studies in the mouse pancreas. Fig. 6, *A–C*, shows that CFTR and NHE3 are co-localized in the luminal membrane of the mouse pancreatic duct. In view of the results in Fig. 5, it was of interest to determine whether EBP50 is also localized at the luminal pole of the pancreatic duct. Fig. 6, *D–F*, shows that EBP50 can be found in the lateral and luminal regions of pancreatic duct cells and that there is substantial co-localization between EBP50 and CFTR in the luminal pole of these cells.

We next determined whether CFTR inhibits the Na^+-dependent H^+ efflux (or OH^- influx) activity in the luminal membrane of the perfused pancreatic duct. We previously showed that 50% of the luminal Na^+-dependent pH_i increase is mediated by NHE3 and about 50% by a novel, Na^+-dependent, and amiloride-sensitive mechanism different from any known NHE isoform (8). The Na^+-dependent pH_i increase was measured in perfused ducts from WT and ΔF mice. Fig. 7*A* shows that exposing the luminal membrane of an acidified duct from the WT pancreas to 140 mM Na^+ resulted in a pH_i recovery at a rate of 1.02 ± 0.09 pH units/min ($n = 13$). The subsequent addition of Na^+ to the bath had no further effect on pH_i, indicating that luminal Na^+ caused maximal recovery of pH_i. As we reported previously (8), stimulation of the duct with forskolin dose-dependently inhibited the luminal Na^+-dependent pH_i recovery in ducts from WT mice.

When the activity of the luminal Na^+-dependent pH_i recovery was measured in pancreatic ducts from ΔF mice, it was immediately evident that the basal activity was significantly lower than that in ducts from WT mice (Fig. 7*B*). In fact, Na^+-dependent pH_i recovery in pancreatic ducts from ΔF mice occurred at a rate of 0.42 ± 0.1 pH units/min ($n = 9$), which is only 40% of that measured in ducts from WT mice. Furthermore, luminal Na^+ only partially recovered pH_i of acidified ducts from ΔF animals and exposing the basolateral membrane of the ducts to Na^+ after completion of luminal-dependent pH_i recovery resulted in an increase in pH_i back to resting levels. In additional experiments, we compared the basolateral Na^+-dependent pH_i recovery of ducts from the pancreas of WT and ΔF mice and found them to be the same (not shown). Hence, only

the luminal Na^+-dependent pH_i recovery was reduced by ~60% in pancreatic ducts from ΔF mice. Another significant finding in Fig. 7*B* and the summary shown in Fig. 7*C* is that forskolin stimulation did not inhibit the residual Na^+-dependent pH_i recovery in the luminal membrane of the pancreatic duct.

The reduction in NHE3 activity in ducts from ΔF animals can be due to down-regulation of NHE3 activity or NHE3 protein expression. To distinguish between these possibilities, we compared the level of NHE3 protein in pancreatic tissues from WT and ΔF mice by Western blot. In nine separate experiments, the Western blotting showed significant variability in the level of NHE3. Examples of preparation from WT and three preparations from ΔF animals are shown in Fig. 8*A*. The levels of NHE3 in tissues from ΔF animals varied between 103 and 28% of WT. This might reflect a variable amount of duct cells, in particular large ducts in preparations. Nevertheless, averaging the nine experiments showed 31 ± 11% ($p = 0.128$) less NHE3 protein in pancreata from ΔF relative to WT mice. More reliable results were obtained when the level of NHE3 expression was analyzed in confocal images collected from ducts stained with two separate anti-NHE3 antibodies. Fig. 8*B* shows that expression of NHE3 protein in the luminal membrane of the pancreatic duct of ΔF mice was markedly reduced. Similar results were obtained with two different Abs (1566 and 1568) that recognize different epitopes of NHE3 and in several pairs of animals of ages ranging between 10 days and 6 months old (not shown). Analysis of 22 images from WT and 20 images from ΔF mice showed that expression of NHE3 was reduced in the luminal membrane of pancreatic ducts from ΔF ducts by 53 ± 4% ($p < 0.01$) (Fig. 8*C*). This reduction does not appear to be due to increased endocytosis of NHE3, since no evidence for an increased intracellular pool of NHE3 could be detected (for example, see Fig. 8*B*). Hence, it seems that CFTR stabilizes expression of NHE3 in the luminal membrane of the pancreatic duct.

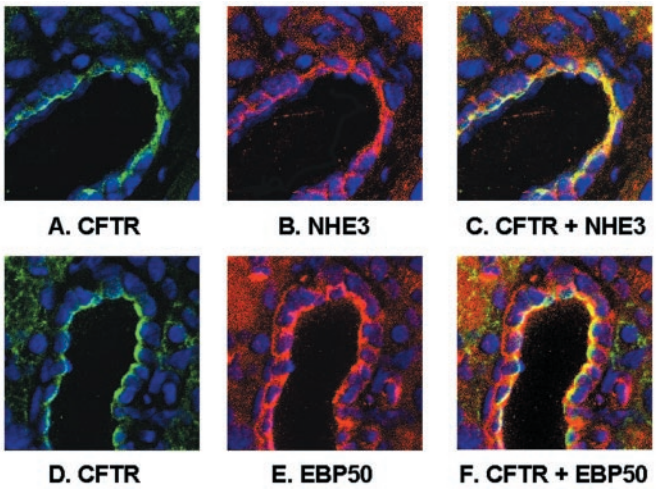

FIG. 6. **Immunolocalization of CFTR, NHE3, and EBP50 in pancreatic ducts.** Frozen sections were prepared from the mouse pancreas, fixed, and double stained with anti-CFTR and anti-NHE3 antibodies (*A–C*) or anti-CFTR and anti-EBP50 antibodies (*D–F*). Similar results were observed in at least four separate experiments.

DISCUSSION

The main function of the pancreatic duct is the secretion of fluid rich in HCO_3^- in response to feeding stimuli such as VIP and secretin. CFTR in the luminal membrane plays a prominent role in HCO_3^- secretion by the stimulated pancreatic duct (6). However, at rest the duct absorbs HCO_3^- to generate a low HCO_3^-, acidic pancreatic juice (28). In previous work, we showed that the mouse pancreatic duct accomplishes HCO_3^- salvage by expressing NHE3 and a novel Na^+-dependent H^+ efflux or OH^- influx mechanisms in the luminal membrane (8). Because both CFTR and NHE3 bind to the scaffolding proteins EBP50 and E3KARP, it was of interest to determine whether CFTR exists in the same complex as NHE3 and whether CFTR can regulate HCO_3^- salvage by inhibiting the activity of NHE3.

In the present work, we studied the regulatory interaction between CFTR and NHE3 in heterologous systems and in the native mouse pancreatic duct. Functional studies, backed by

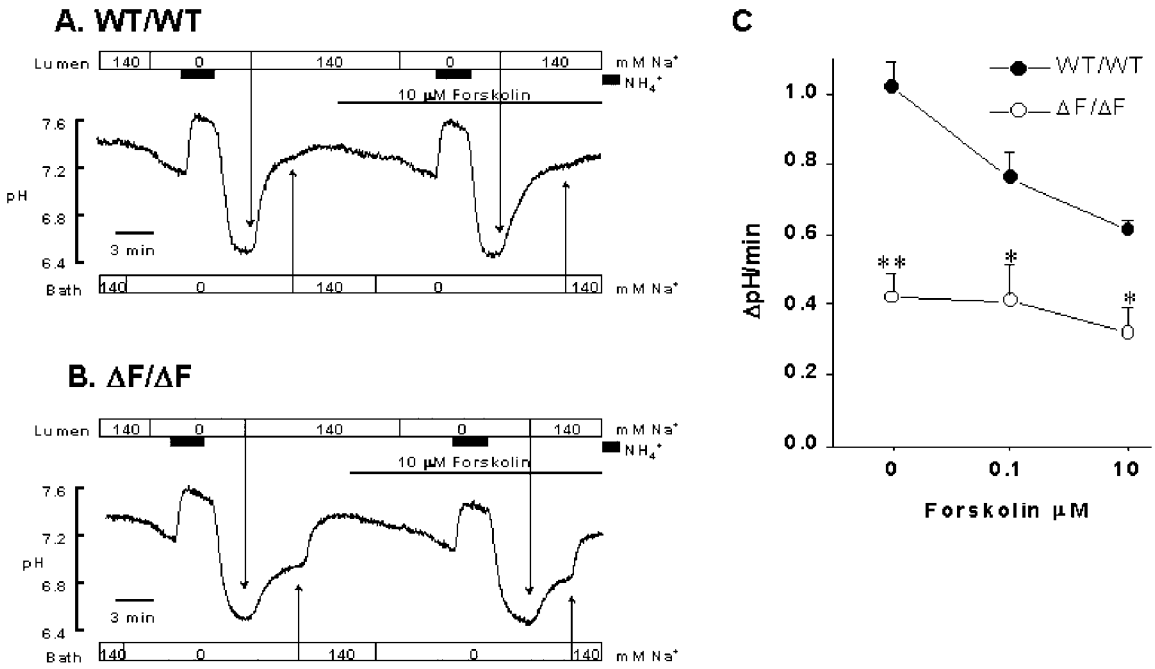

FIG. 7. **NHE activity in the luminal membrane of pancreatic ducts from WT and ΔF mice.** Pancreatic ducts were microdissected from WT (*A*) and ΔF mice (*B*), cannulated, and used to measure luminal Na^+-dependent recovery from an acid load before and after forskolin stimulation of the same ducts. In all experiments, the effect of basolateral Na^+ on pH_i recovery was measured after measurement of the luminal activity under resting conditions. The results of multiple experiments are summarized in *C*. **, $p < 0.01$; *, $p < 0.05$ compared with control.

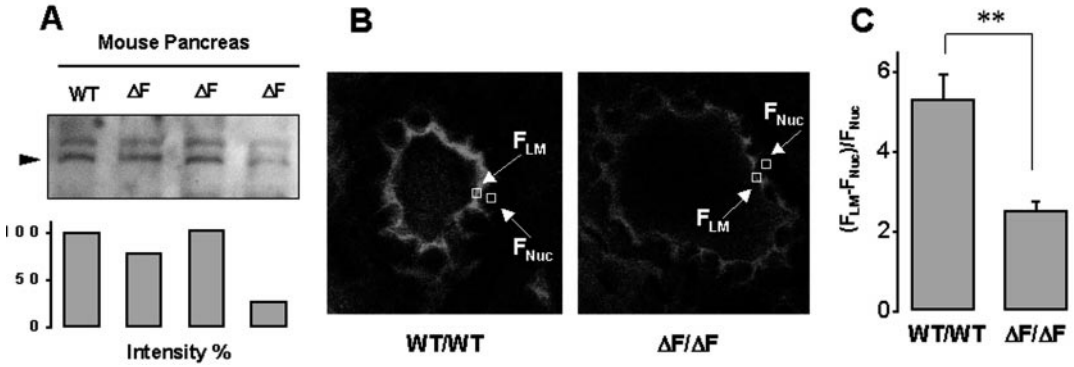

FIG. 8. **Analyses of NHE3 expression in pancreatic ducts from WT and ΔF mice.** The main pancreatic ducts were dissected from WT and ΔF mice and used for Western blot analysis of NHE3 (*A*). Band intensities were determined by densitometry. In the second protocol, frozen sections were prepared from the mouse pancreas of WT and ΔF mice, fixed, and stained with anti-NHE3 antibodies (*B*). The sections were used to measure intensity of NHE3 staining in the nuclear (background) and luminal membrane (experimental) regions, as marked in *B*. Results of all experiments are summarized in *C*. **, $p < 0.01$ compared with control.

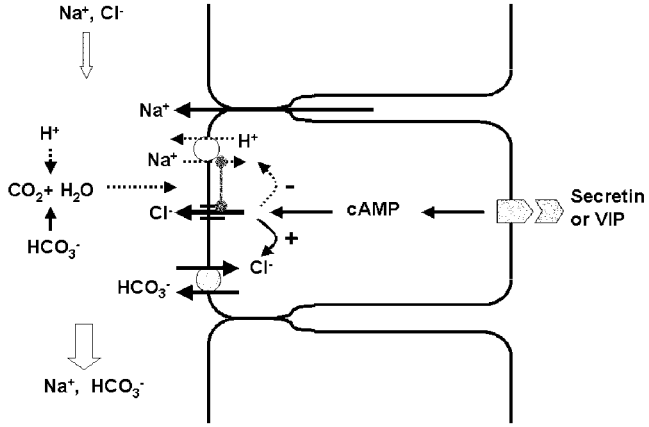

FIG. 9. **A model of** HCO_3^- homeostasis in the resting and stimulated pancreatic duct. In the resting state, CFTR (and possibly EBP50) does not interact with the HCO_3^- salvage mechanisms, which operates at maximal capacity. Upon cell stimulation, CFTR, EBP50, and NHE3 are assembled into a complex to inhibit HCO_3^- salvage and at the same time stimulate HCO_3^- secretion.

molecular, biochemical, and immunocytological evidence suggest that CFTR controls NHE3 activity by two mechanisms: 1) CFTR increases expression of NHE3 in the luminal membrane of the pancreatic duct, and 2) CFTR acutely augments the cAMP-dependent inhibition of NHE3.

Probably the most striking finding of the present work is the reduced levels of NHE3 protein and activity in the pancreatic duct of ΔF mouse. Reduced expression of NHE3 was observed by Western blot and by reduced staining of the luminal membrane of the duct. Furthermore, measurement of total Na^+-dependent recovery from acidification revealed nearly 60% reduction in the rate of pH_i recovery in ducts of ΔF mice. Reduced expression of NHE3 in the pancreatic duct was observed in mice as young as 10 days old. In our colony, 57% of ΔF mice died between 3 weeks and 3 months of age, while the surviving mice lived well for at least 6 months. The pancreatic duct of ΔF mice of all ages showed reduced NHE3 activity relative to the ducts of age-matched WT mice. This suggests that reduction in NHE3 expression in the ΔF mice occurs early in development rather than being an adaptive response to the lack of function of CFTR.

The age-independent reduction in NHE3 expression in ducts of ΔF mice suggests that the most plausible mechanism for control of NHE3 expression by CFTR is stabilization of NHE3 protein expression. CFTR may increase transcription of NHE3 mRNA or the half-life of NHE3 mRNA to increase expression of the protein. Alternatively, by forming a complex including CFTR, EBP50, and NHE3, CFTR may enhance the stability of the expressed NHE3 by either preventing its degradation or by enhancing its delivery to the luminal membrane of the pancreatic duct. It is interesting to note that expression of CFTR in the PS120/NHE3 cells had no measurable effect on the levels of NHE3 protein or on basal NHE3 activity in these cells (Figs. 2 and 4). Hence, of the acute and chronic regulation of NHE3 activity by CFTR *in vivo*, only the acute regulation could be reproduced *in vitro*. This may reflect differences in sorting mechanisms and/or targeted expression of NHE3 between the *in vivo* (pancreas) and model systems (PS120/NHE3 cells) and highlight the importance of confirming observations made in model systems in the *in vivo* situation.

In addition to increasing NHE3 expression in the luminal membrane of the pancreatic duct, CFTR acutely augments the inhibition of NHE3 activity by a cAMP-dependent mechanism. The present work provides evidence to show that such a regulation is mediated by binding of CFTR and NHE3 to EBP50 or other related PDZ scaffolding proteins. Formation of the CFTR·NHE3 complex was dependent on an intact PDZ binding motif of CFTR (Fig. 5), and EBP50, as well as CFTR and NHE3, was co-localized at the luminal pole of pancreatic ducts (Fig. 6). EBP50 has two PDZ domains and an ERM-binding domain. CFTR binds to PDZ1, (10), while NHE3 binds the C terminus of EBP50 including PDZ2 (11). In PS120 fibroblasts, EBP50 was required for cAMP-induced inhibition of NHE3 (13). The present work extends these findings to show that stimulation of CFTR with cAMP further inhibits NHE3 activity, beyond the inhibition of NHE3 activity observed in cells expressing NHE3 and EBP50 alone (Figs. 3 and 4). The EBP50-associated protein ezrin is known to possess an amphipathic helix that can associate *in vitro* with the regulatory subunit of protein kinase A (29). Therefore, it will be interesting to determine whether protein kinase A is indeed contained within CFTR·NHE3 protein complexes by association with ezrin or other cellular A kinase anchoring proteins. In addition, it will be important to identify other activities that require the presence of EBP50, E3KARP, or PDZK1, since these proteins appear to be expressed in excess over the ion channels and transporters whose activities they are known to regulate.

Measurement of Na^+-dependent H^+/OH^- fluxes showed that the pancreatic duct of ΔF mice retained only 40% of the activity measured in ducts from WT mice. In the WT duct, NHE3 mediates only 50% of NHE activity, whereas the remaining activity is mediated by a novel Na^+-dependent mechanism (8). Furthermore, the residual NHE3 expressed in the duct of ΔF

mice is likely to mediate part of the residual luminal NHE activity. This suggests that CFTR regulates the expression and/or activity of both NHE3 and the novel Na^+-dependent H^+/OH^- transport mechanism in the luminal membrane of the pancreatic duct. Once this mechanism is identified with certainty, it will be of particular interest to determine whether it is indeed regulated by CFTR.

The physiological significance of regulating the overall Na^+-dependent HCO_3^- salvage and secretory mechanisms by CFTR is depicted in Fig. 9. Pancreatic ductal fluid and HCO_3^- secretion is stimulated by the G_s-coupled secretin or VIP receptors. Under basal conditions, CFTR is not phosphorylated and does not inhibit the Na^+-dependent HCO_3^- salvage mechanisms. Therefore, HCO_3^- salvage is maximal and produces the small volume of the acidic pancreatic juice. When cells are stimulated, cellular cAMP is increased, and the CFTR·EBP50·NHE3 complex (and possibly the novel Na^+-dependent HCO_3^- salvage mechanism) is formed, modified by other protein associations, or undergoes a conformational change to allow regulatory inhibition of Na^+-dependent H^+/OH^- fluxes by CFTR. At the same time, CFTR stimulates HCO_3^- secretion by activating a Cl^-/HCO_3^- exchange process (5, 7) in the luminal membrane of the pancreatic duct (6). The overall result is production of an alkaline pancreatic juice.

The present findings may have significant importance in understanding the overall role of CFTR in epithelial physiology and in CF. Not only do we report a new role for CFTR in regulating HCO_3^- transport, but we show that CFTR increases expression of H^+/OH^- transport proteins in the luminal membrane of the pancreatic duct. In this respect, recently Wheat *et al.* (30) reported that CFTR up-regulates mRNA expression of the colonic Cl^-/HCO_3^- exchanger DRA (down regulated in adenoma in a model system. The regulation of gene expression adds to the complexity by which CFTR controls overall fluid and electrolyte secretion and further indicates that the loss of CFTR cannot be replaced by activation of alternative Cl^- channels. Rather, the more we understand the role of CFTR in epithelial transport, the more it becomes evident that expression of CFTR in the luminal membrane of fluid-secreting epithelia is critical for epithelial cell function and normal fluid-electrolyte homeostasis.

REFERENCES

1. Johansen, P. G., Anderson, C. M., and Hadorn, B. (1968) *Lancet* **1,** 455–460
2. Pilewski, J. M., and Frizzell, R. A. (1999) *Physiol. Rev.* **79,** S215–S255
3. Vankeerberghen, A., Wei, L., Jaspers, M., Cassiman, J. J., Nilius, B., and Cuppens, H. (1998) *Hum. Mol. Genet.* **7,** 1761–1769
4. Stutts, M. J., Canessa, C. M., Olsen, J. C., Hamrick, M., Cohn, J. A., Rossier, B. C., and Boucher, R. C. (1995) *Science* **269,** 847–850
5. Lee, M. G., Wigley, W. C., Zeng, W., Noel, L. E., Marino, C. R., Thomas, P. J., and Muallem, S. (1999) *J. Biol. Chem.* **274,** 3414–3421
6. Lee, M. G., Choi, J. Y., Luo, X., Strickland E., Thomas, P. J., and Muallem, S. (1999) *J. Biol. Chem.* **274,** 14670–14677
7. Choi, J. Y., Muallem, D. Kiselyov, K. Lee, M. G., Thomas, P. J., and Muallem, S. (2001) *Nature*, **410,** 94–97
8. Lee, M. G., Ahn, W., Choi, J. Y., Luo, X., Seo, J. T., Schultheis, P. J., Shull, G. E., Kim, K. H., and Muallem, S. (2000) *J. Clin. Invest.* **105,** 1651–1658
9. Choi, J. Y., Shah, M., Lee, M. G., Schultheis, P. J., Shull, G. E., Muallem. S., and Baum, M. (2000) *J. Clin. Invest.* **105,** 1141–1146
10. Short, D. B., Trotter, K. W., Reczek, D., Kreda, S. M., Bretscher, A., Boucher, R. C., Stutts, M. J., and Milgram, S. L. (1998) *J. Biol. Chem.* **273,** 19797–19801
11. Weinman, E. J., Steplock, D., Tate, K., Hall, R. A., Spurney, R. F., Shenolikar, S. (1998) *J. Clin. Invest.* **101,** 2199–2206
12. Sun, F., Hug, M. J., Lewarchik, C. M., Yun, C., Bradbury, N. A., and Frizzell, R. A. (2000) *J. Biol. Chem.* **275,** 29539–29546
13. Yun, C. H. C., Oh, S., Zizak, M., Steplock, D., Tsao, S., Tse, C. M., Weinman, E. J., and Donowitz, M. (1997) *Proc. Natl. Acad. Sci. U. S. A.* **94,** 3010–3015
14. Lamprecht, G., Weinman, E. J., Yun, C. H. C. (1998) *J. Biol. Chem.* **273,** 29972–29978
15. Mohler, P. J., Kreda, S. M., Boucher, R. C., Sudol, M., Stutts, M. J., and Milgram, S. L. (1999) *J. Cell Biol.* **147,** 879–890
16. Amemiya, M., Loffing, J., Lotscher, M., Kaissling, B., Alpern, R. J., and Moe, O. W. (1995) *Kidney Int.* **48,** 1206–1215
17. Pouyssegur, J., Sardet, C., Franchi, A., L'Allemain, G., and Paris, S. (1984) *Proc. Natl. Acad. Sci. U. S. A.* **81,** 4833–4837
18. Park, K., Olschowska, J. A., Richardson, L. A., Bookstein, C., Chang, E. B., and Melvin, J. E. (1999) *Am. J. Physiol.* **39,** G470–G478
19. Wakabayashi, S., Fafournoux, P., Sardet, C., and Pouyssegur, J. (1992) *Proc. Natl. Acad. Sci. U. S. A.* **89,** 2424–2428
20. Kocher, O., Comella, N., Tognazzi, K., and Brown, L. F. (1998) *Lab. Invest.* **78,** 117–125
21. Zeiher, B. G., Eichwald, E., Zabner, J., Smith, J. J., Puga, A. P., McCray, P. B. Jr., Capecchi, M. R., Welsh, M. J., and Thomas, K. R. (1995) *J. Clin. Invest.* **96,** 2051–2064
22. Zeng, W., Lee, M. G., Yan, M., Diaz, J., Benjamin, I., Marino, C. R., Kopito, R., Freedman, S., Cotton, C., Muallem, S., and Thomas, P. J. (1997) *Am. J. Physiol.* **273,** C442–C455
23. Lee, M. G., Schultheis, P. J., Yan, M., Shull, G. E., Bookstein, C., Chang, E., Tse, M., Donowitz, M., Park, K., and Muallem, S. (1998) *J. Physiol.* (*Lond.*) **513,** 341–357
24. Wang, S., Yue, H., Derin, R. B., Guggino, W. B., and Li, M. (2000) *Cell* **103,** 169–179
25. Zhang, L., Wang, D., Fischer, H., Fan, P. D., Widdicombe, J. H., Kan, Y. W., and Dong, J. Y. (1998) *Proc. Natl. Acad. Sci. U. S. A.* **95,** 10158–10163
26. Mickle, J. E., Macek, M., Jr., Fulmer-Smentek, S. B., Egan, M. M., Schwiebert, E., Guggino, W., Moss, R., and Cutting, G. R. (1998) *Hum. Mol. Genet.* **7,** 729–735
27. Moyer, B. D., Denton, J., Karlson, K. H., Reynolds, D., Wang, S., Mickle, J. E., Milewski, M., Cutting, G. R., Guggino, W. B., Li, M., and Stanton, B. A. (1999) *J. Clin. Invest.* **104,** 1353–1361
28. Owyang, C., and Williams, J. A. (1995) in *Textbook of Gastroenterology* (Yamada, T., eds) 2nd Ed., pp. 361–383, J. B. Lippincott Co., Philadelphia
29. Dransfield, D. T., Bradford, A. J., Smith, J., Martin, M., Roy, C., Mangeat, P. H., and Goldenring, J. R. (1997) *EMBO J.* **16,** 35–43
30. Wheat, V. J., Shumaker, H., Burnham, C., Shull, G. E., Yankaskas, J. R., and Soleimani, M. (2000) *Am. J. Physiol. Cell Physiol.* **279,** C62–C71